Positive Pion Production in Proton-Proton Collisions at 450 Mev*†

LEE G. PONDROM‡§
Enrico Fermi Institute for Nuclear Studies, University of Chicago, Chicago, Illinois
(Received January 28, 1959)

The external proton beam of the Chicago cyclotron has been used to study the reaction $p+p \rightarrow \pi^+ + n + p$ at 450 Mev. The reaction $p+p \rightarrow \pi^+ + d$ was also measured as a check on the equipment. A double focusing wedge magnet was used to observe the momentum distribution of pions at angles of 14°, 20.5°, and 30° in the laboratory system. The over-all resolution of the magnet system varied from 1.5% to 2.2%. A least squares fit of the $p+p \rightarrow \pi^+ + d$ data in the center-of-mass system gives $d\sigma/d\Omega \propto (0.38 \pm 0.20 + \cos^2\theta)$ with $\sigma = 1.47 \pm 0.12$ millibarns. The spectra for the unbound reaction were fitted to *Ss*, *Sp*, *Ps*, and *Pp* spectrum shapes predicted by the phenomenological theory of pion production. This fit gives $d\sigma/d\Omega \propto (0.40 \pm 0.08 + \cos^2\theta)$ with $\sigma = 1.80 \pm 0.7$ millibarns. The results of this fit have been compared with the cross section for neutral pion production at 450 Mev. This comparison was found satisfactory for the amounts of the *Ss*, *Sp*, and *Pp* spectrum shapes found in this experiment, but an excessively large amount of the *Ps* shape, 0.38 ± 0.10 millibarns, was required to fit the data. The results show that $\sigma_{10}(Pp)$ is much smaller than has been previously reported. An excitation function for the unbound cross section is predicted by this fit in terms of the phenomenological model, and is found to increase too rapidly at high bombarding energies.

INTRODUCTION

THERE has been interest in single meson production in nucleon-nucleon collisions both at high and low bombarding energies since the review article by Rosenfeld in 1954.[1] High bombarding energy is characterized by a pion kinetic energy well above the 120-Mev resonance. The experimental data on the pion energy spectra from the reaction

$$p+p \rightarrow \pi^+ + n + p, \tag{1}$$

at high energy has been satisfactorily explained by the isobaric nucleon model of Lindenbaum and Sternheimer.[2] In this model nucleon-nucleon interactions are ignored in the final state, and a nucleon-isobar configuration is assumed to decay into two nucleons and a pion.

Mescheryakov *et al.*[3] have made careful measurements of the pion spectra from reaction (1) at 24° in the lab at the intermediate energies of 556 and 660 Mev. They find satisfactory agreement with the observed shapes by ignoring final state nucleon-nucleon interactions, and by assuming a production matrix element proportional to p, the pion momentum. The excitation function and total cross section for reaction (1) have been measured by Dzhelepov *et al.*[4] and more accurately by Neganov and Savchenko[5] in the bombarding energy region from 470 to 660 Mev.

At energies near threshold, where the maximum pion energy available is well below the 120-Mev resonance, the phenomenological theory of Brueckner and Watson should be valid.[6] This theory ignores the pion-nucleon interaction and treats the np interaction in terms of effective range theory for the ^3S state. Only s and p angular momentum states are considered for the np and pion systems because of the long particle wave lengths with respect to the radius of the interaction volume. This gives four possible combinations: *Ss*, *Sp*, *Ps*, and *Pp*; the capital letter refers to the angular momentum of the two nucleon system, and the small letter refers to the angular momentum of the pion with respect to the center of mass. The *Ss* and *Sp* states are connected by this theory to the s and p state terms in the cross section for the reaction

$$p+p \rightarrow \pi^+ + d, \tag{2}$$

which has an excitation function near threshold of the form

$$\sigma_{10}(d) = \alpha\eta + \beta\eta^3. \tag{3}$$

Here $\alpha\eta$ represents s state, and $\beta\eta^3$ represents p state contributions. The *Ps* and *Pp* states of reaction (1) are connected by isotopic spin conservation to the identical states in the reaction

$$p+p \rightarrow \pi^0 + p + p. \tag{4}$$

The experiment of Rosenfeld[7] was analyzed in terms of *Ss* and *Sp* for reaction (1), although such analysis did not give agreement between the cross sections for reactions (1) and (2). Alston *et al.*[8] at 383 Mev observed the spectrum from reaction (1) and the bound to

* Research supported by a joint program of the Office of Naval Research and the U. S. Atomic Energy Commission.
† A thesis submitted to the Department of Physics, the University of Chicago, in partial fulfillment of the requirements for the Ph.D. degree.
‡ National Science Foundation Predoctoral Fellow, 1957–1958.
§ Now at the Aeronautical Research Laboratory, Wright-Patterson Air Force Base, Ohio.
[1] A. H. Rosenfeld, Phys. Rev. **96**, 139 (1954).
[2] S. J. Lindenbaum and R. M. Sternheimer, Phys. Rev. **105**, 1874 (1957). See this paper for experimental references.
[3] Meshcheryakov, Zrelov, Neganov, Vzorov, and Shabudin, J. Exptl. Theoret. Phys. U.S.S.R. **31**, 45 (1956) [translation: Soviet Phys. JETP **4**, 60 (1957)].
[4] Dzhelepov, Moskalev, and Medved, Doklady Akad. Nauk S.S.S.R. **104**, 380 (1955).
[5] B. S. Neganov and O. V. Savchenko, J. Exptl. Theoret. Phys. U.S.S.R. **32**, 1265 (1957) [translation: Soviet Phys. JETP **5**, 1033 (1957)].
[6] K. M. Watson and K. A. Brueckner, Phys. Rev. **83**, 1 (1951). See also M. Gell-Mann and K. M. Watson, *Annual Reviews of Nuclear Science* (Annual Reviews, Inc., Stanford, 1956), Vol. IV, p. 219.
[7] A. H. Rosenfeld, Phys. Rev. **96**, 130 (1954).
[8] Alston, Crewe, Evans, and von Gierke, Proc. Phys. Soc. (London) **A69**, 691 (1956).

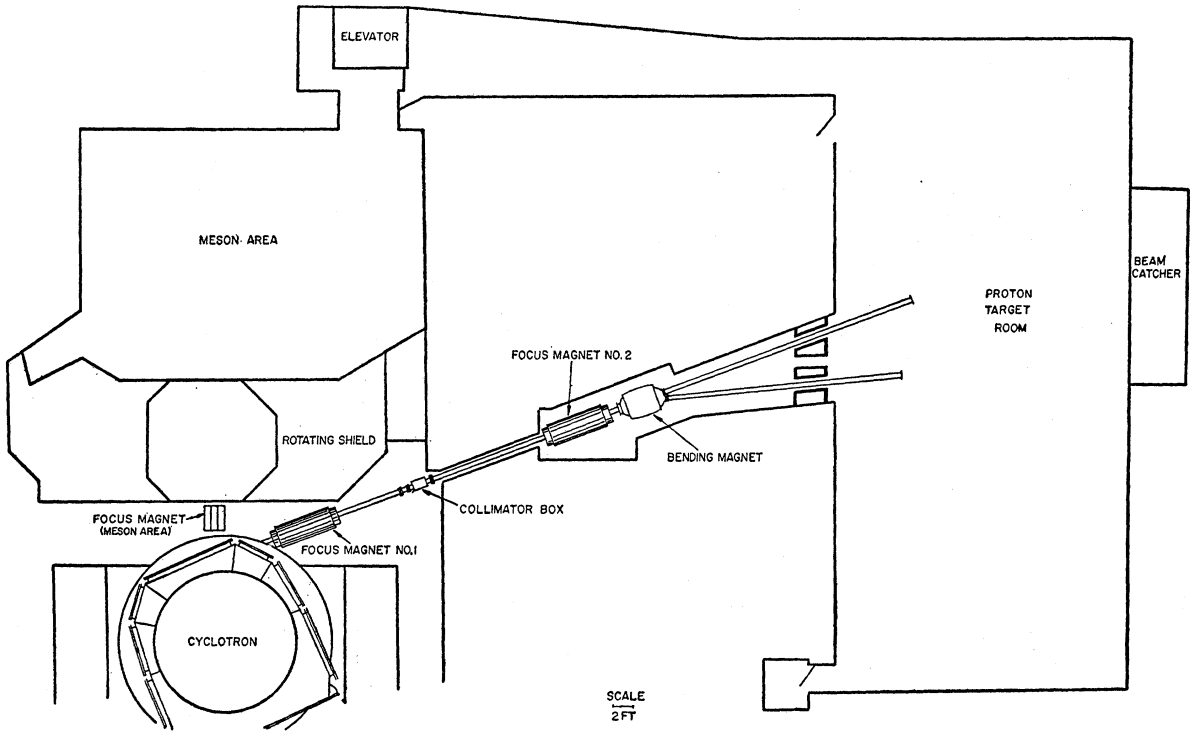

FIG. 1. Cyclotron and external proton beam facilities. The targets were placed in front of the aluminum window on the undeflected beam line. The beam spot at this point was typically $\frac{1}{2}$ in.$\times$1 in.

unbound ratio, and found that agreement with the phenomenological theory could be obtained by adding a Pp term to the cross section for the unbound reaction.

The coefficients in Eq. (3) have been determined to 10% by Crawford and Stevenson.[9] This fit agrees with the experimental cross section for pion energies up to 80 Mev in the center of mass.[10] Reaction (4) has been studied near threshold by Moyer and Squire,[11] and from 346 to 437 Mev by Stallwood.[12] With these data, and the phenomenological model, one can predict the relative contributions that the Ss, Sp, Ps, and Pp spectrum shapes should make in the observed spectrum from reaction (1).

II. EXPERIMENTAL EQUIPMENT

A. External Beam and Monitoring

The extraction of the external beam of the Chicago cyclotron has been described elsewhere.[13] The layout of the proton target station and the beam control magnets are shown in Fig. 1. The focusing magnets are three section quadrupoles, with differential excitation of the center section to produce an anastigmatic focus. Collimators can be inserted in the beam at the cross over point between the two focusing magnets. The bending magnet was not used in the present experiment. The beam travels from the cyclotron through the three magnets and into the target station inside a six inch aluminum vacuum pipe, which is normally connected directly onto the cyclotron vacuum system. After extraction, the beam is focused by adjusting the excitation of the focusing magnets while observing the beam spot on an x-ray intensifier screen at the target position. The spot is viewed remotely through a telescope. Then the exact path of the beam is found by exposing photographic enlarging paper for a few minutes at different points along the beam line.

The proton beam was monitored by a secondary emission monitor (SEM) of the Tautfest type.[14] This monitor has the advantage over an ionization chamber that it does not saturate in output current at very high beam current densities. The output current from the collector plates of the monitor was integrated into a total charge by a polystyrene capacitor on the input of an electrometer. The electrometer was a vibrating reed type made by the Applied Physics Corporation. The output current of the vibrating reed was observed remotely on a Brown Multiple Range recorder. The drift current of the instrument corresponded to a proton flux of about 10^5

[9] Frank S. Crawford, Jr., and M. Lynn Stevenson, Phys. Rev. **97**, 1305 (1955).
[10] See, for example, Charles E. Cohn, Phys. Rev. **105**, 1582 (1957).
[11] Burton J. Moyer and Robert K. Squire, Phys. Rev. **107**, 283 (1957).
[12] Stallwood, Sutton, Fields, Fox, and Kane, Phys. Rev. **109**, 1716 (1958).
[13] A. V. Crewe and U. E. Kruse, Rev. Sci. Instr. **27**, 5 (1956).
[14] G. W. Tautfest and H. R. Fechter, Rev. Sci. Instr. **26**, 229 (1955).

protons per second. The output current of the monitor was independent of the bias voltage on the bias plates for voltages between 20 and 45 volts. The SEM was calibrated by establishing a ratio between its reading and the reading of an argon filled ionization chamber (IC) in the same beam. The IC was calibrated with scintillation counters by establishing counting ratios between counters in the beam and counters looking at the beam after multiple scattering in 2 in. of lead. This was necessary because the IC drift current was 10^3 protons/sec, and the large beam duty cycle (1600) required a maximum safe scintillation counting rate of about 10^2 protons/sec. The ion chamber calibration gave 183 ± 4 ion pairs per centimeter in argon for 452-Mev protons; the gas pressure was 95.4 cm, and the temperature was 20°C. This result agrees well with the result of Bakker and Segrè[15] at 340 Mev, which, when scaled up to our energy, temperature, and pressure gives 177 ion pairs/cm. At a beam intensity between 10^7 and 10^8 protons/sec both the SEM and the IC could be safely operated, and a ratio of the two output currents was established. This ratio was re-checked at the end of the experiment, and found to be the same to about 1%. The result gave a sensitivity of $S=(5.12\pm0.15)\times10^{10}$ protons/3 volts with a 0.001 microfarad capacitor on the input, or a multiplication efficiency for the chamber of 0.366 electrons per proton.

A Bragg curve was run by placing copper absorbers between the SEM and the IC, and observing the ratio of the output currents, IC/SEM. In interpreting these data we followed the analysis of Mather and Segrè[16]; we corrected for multiple scattering and for the error in the mean excitation potential for copper, as discussed in the range-energy tables of Rich and Madey.[17] This procedure yielded a beam energy after passing through the SEM of 452.4 ± 0.5 Mev.

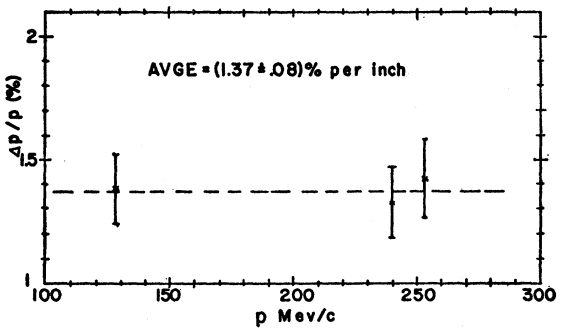

FIG. 2. Measurements of momentum dispersion for the spectrometer at three different momenta. The 128 Mev/c point comes from alpha-particle data. The two high momentum points are the results of measurements with pions.

[15] C. J. Bakker and E. Segrè, Phys. Rev. **81**, 489 (1951).
[16] R. L. Mather and E. Segrè, Phys. Rev. **84**, 181 (1951).
[17] Marvin Rich and Richard Madey, U. S. Atomic Energy Commission, University of California Radiation Laboratory Report UCRL-2301, 1954 (unpublished).

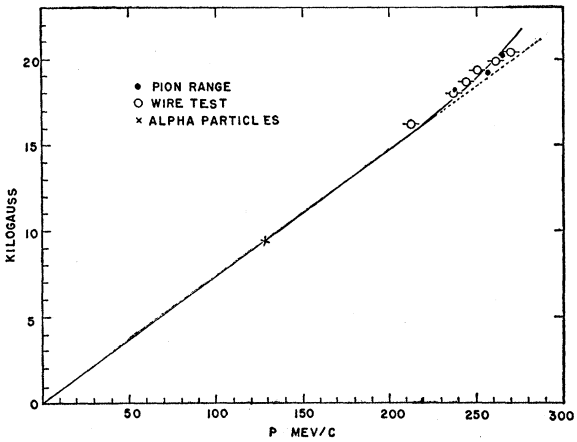

FIG. 3. Momentum *versus* central field for the spectrometer orbit.

B. Spectrometer and Counting Equipment

The standard meson beam steering magnet at the Chicago cyclotron, described by Wright and Warshaw,[18] was used as a double focusing wedge magnetic spectrometer. Because of the large ratio of fringe field to central field in this magnet, a total bending angle of 69° with a 24° wedge was required to achieve vertical focus. The radial and vertical focusing properties of the system and the momentum dispersion and solid angle transmission were checked at 128 Mev/c by using 8.78-Mev alpha particles from ThC′. Focus and dispersion properties were later checked up to 260 Mev/c using pions from reaction (2). Figure 2 shows the momentum dispersion results. The p *versus* B curve for the spectrometer, Fig. 3, was obtained from the alpha particle runs, the average of several floating wire tests, and range curves on the pions from reaction (2). The central magnetic field was measured during the experiment by a null-balancing flip coil circuit which used an air core solenoid as a reference. This instrument was calibrated with a Numar Precision Gaussmeter, a nuclear resonance device. The reproducibility of the readings was about 0.3%. The magnet was excited by a 300 kilowatt motor-generator set, which was regulated to 0.1% by a dc amplifier feedback system.

Figure 4 gives an over-all view of the experimental equipment in the proton target room. The defining slits shown on the input side of the spectrometer were 50 in. from the target, and were the only slits used in the system. The slit opening, 2 in. by $1\frac{1}{2}$ in., was known to have 100% transmission at low momenta from the alpha particle runs. The defining jaws were $\frac{3}{4}$ in. square tungsten blocks. The solid angle was checked in the radial direction by decreasing the radial opening to 1 in., and observing the corresponding decrease in the net carbon rate. This check was satisfactory to a 4% statistical accuracy. This also served to show that slit scattering effects were not important. The magnet and

[18] S. C. Wright and S. D. Warshaw (unpublished).

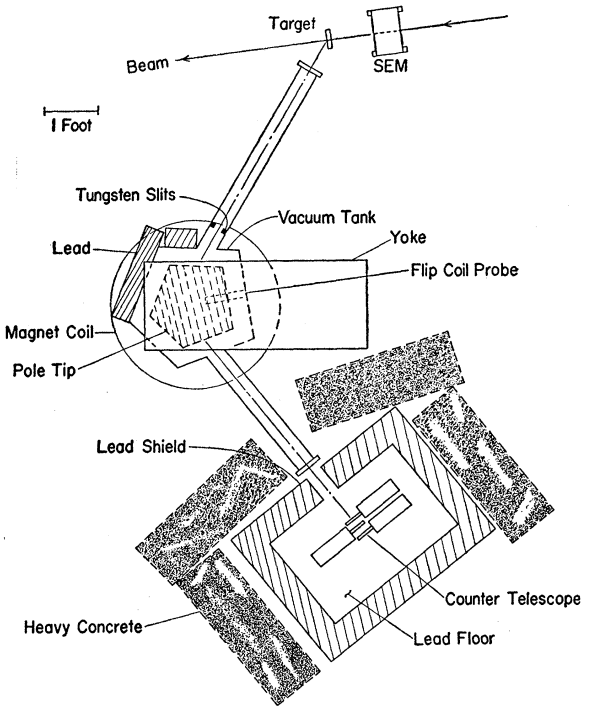

FIG. 4. Experimental setup in the proton target room.

counting system were carefully aligned at each lab angle by an optical procedure using mirrors and a transit. This alignment was checked by doing an up-down scan at the counter telescope with a $\frac{1}{2}$-in. square counter; this test also checked the vertical focus, and showed that a 2-in. high defining counter collected all of the beam. To facilitate angle changes, the magnet and counter house could be rotated about a pin under the target.

The triples counting telescope was a standard design, using plastic scintillators and 6810 phototubes. The defining counter was $\frac{1}{2}$ in. wide and 2 in. high, giving a momentum resolution of $\Delta p/p=0.7\%$. This counter had an air light pipe to avoid the possibility of Čerenkov radiation in a Lucite pipe. To cut down accidentals, $\frac{1}{16}$ in. of copper was normally kept between counters 1 and 2, and between 2 and 3. The calculated collection efficiency of the counters for pions multiply-Coulomb scattered in traversing the telescope was greater than 98% for pion energies down to 45 Mev. Modified Garwin circuits were used by the coincidence equipment. The system was aligned before each run by checking phototube voltage plateaus and relative delays. The effectiveness of the shielding was checked by observing the rate dependence of double and triple coincidences. Counter efficiencies were periodically checked by placing one $\frac{1}{4}$-in. by 1-in. counter on either side of the telescope. The triple coincidence efficiency was always found to be 98% or greater. The calculated cut-off energy of the telescope was 35 Mev for pions. Checks for pion loss at the low energy spectrum points (45 Mev to 40 Mev) were made by varying the absorber in the telescope, and no losses were observed, although the statistical accuracy of the low energy results was poor—from 15% to 20%.

C. Targets

Hydrogen rates were measured by taking CH_2-C differences. The CH_2 target was carefully machined to a nominal $\frac{1}{2}$ in. thickness, and was of a very uniform volume density. The carbon target was machined to a nominal $\frac{1}{4}$ in. thickness, and came from a graphite sample of uniform density to about 0.1%. The surface densities were 1.177 g/cm^2 for the CH_2 and 1.014 g/cm^2 for the graphite. This gives a ratio of carbon atoms per cm^2 in the two targets of (C in CH_2/C in C)$=0.995$. Thus the number of carbon atoms was the same in each target to 0.5%, and empties rates were not needed in the subtraction. These measured predictions were checked experimentally to 3% by observing negative pions from the two targets. Crewe has recently confirmed the thickness measurements to 0.5% by analyzing p-p scattering with a magnetic spectrometer.[19] Since the two targets had equal numbers of carbon atoms per cm^2, the CH_2 target had a larger stopping power for pions than the graphite target. The difference in half thickness amounted only to 0.5 Mev, however, and did not effect the spectrum measurements.

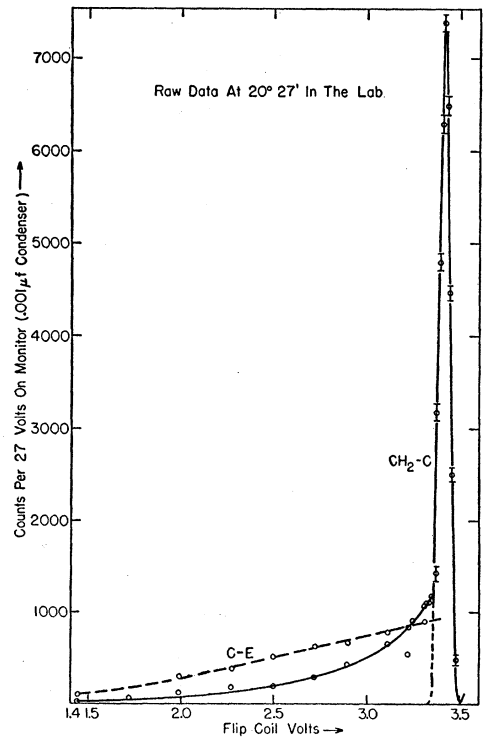

FIG. 5. Complete peak and continuum data at 20.5°. The carbon spectrum is sketched in for comparison. The small rise above 3.5 flip coil volts indicates reflection scattering of pions off of the vacuum system.

[19] A. V. Crewe (private communication).

III. RESULTS

A. Data Reduction Procedure

Figure 5 shows the spectrum data from the 20.5° run. Each run required about 18 hours, and was made from high momenta to low momenta. After completing the run the peak and continuum beginning were re-scanned as a check. In order to convert the data into differential cross sections, several systematic corrections were made.

The muon contamination of the peaks was concluded to be 2% or less on the basis of a careful range curve run at 30°; such a small contamination was negligible. The positron contamination of both the peaks and the continua was concluded to be negligible on the basis of the negative pion runs, which were originally made to check the carbon subtraction. No range curves were attempted on the continuous spectra because of the very low counting rates, so that the muon contamination had to be estimated. The continua could be contaminated either by muons from the decay of pions in the region of the target (similar to the source of most of the muon contamination of cyclotron pion beams), or from the large flux of pions coming out of the exit face of the magnet. With the continuum filling the exit pipe, the total muon contribution was estimated to be from 2% to 3%, and roughly energy independent. Because of the reasonably good definition of the magnet system, only a volume of radius 6 in. near the target was available for the emission of muons into the spectrometer. This contamination was calculated, using monoenergetic pions of the peak energy from reaction (2), isotropically distributed about the 10° half angle with respect to the input axis of the magnet. The correction was found to be as high as 6% for the low-energy continuum points. In applying the pion decay correction, the total path length from target to counters of 130 in. was used; the pion lifetime was taken to be $\tau=2.56\pm0.05\times10^{-8}$ sec.[20]

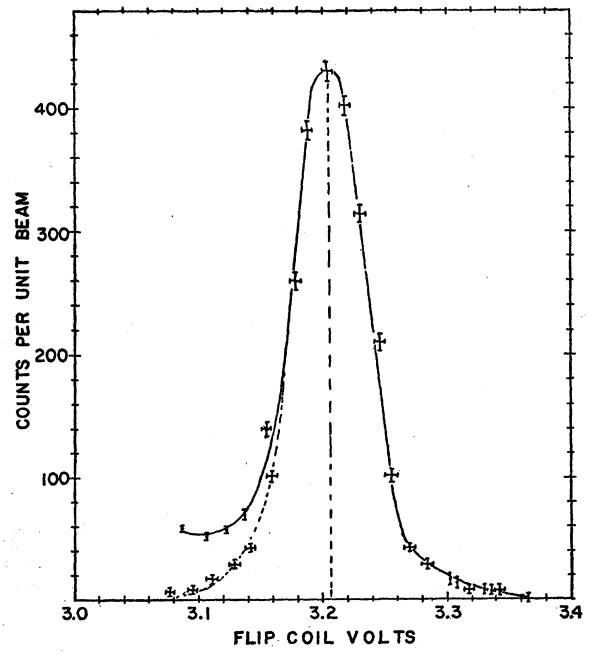

FIG. 6. Peak from $p+p\rightarrow\pi^{+}+d$ and continuum beginning at 30°. The dotted tail at lower fields represents the results of symmetrizing the peak about its center line.

In calculating the absorption of pions by the hydrogen in the CH_2 target and by the first two counters, the $\pi^{+}p$ total cross section and its energy dependence were taken into account. For the carbon in these materials, and for the copper in the counter telescope, the total cross section was assumed to be geometrical, and a nuclear radius $r_0=1.2A^{\frac{1}{3}}\times10^{-13}$ cm was used. The best average value of the three points of Fig. 3, $\Delta p/p=(0.0137\pm0.0008)$ per inch, was used in analyzing all of the data. The defining counter width was in fact 0.495 in., giving $\Delta p/p=(0.68\pm0.04)\%$ for the counter telescope. Good phototube plateaus were always obtained, and no evidence was found of an effective counter width for this counter less than the physical width.

Multiple scattering of pions in the CH_2 caused an uncertainty in the lab angle, and a corresponding uncertainty in the center-of-mass angle. At low energies the total center of mass spread, including the 2.3° defining lab angle, amounted to ±5°. Assuming $d\sigma/d\Omega$ to vary linearly over this range, the correct average center-of-mass angle was simply the calculated angle. The low energy data covered a 30° range of center-of-mass angles. This was thought sufficient to detect the angular distribution of the form $A+\cos^2\theta$, and the effect of multiple scattering was ignored. Evidence of reflection scattering of peak pions from the 4-in. diameter aluminum vacuum pipe on the magnet output face was found on the high momentum side of the 20.5° peak, as indicated in Fig. 5. About 0.4% of the total peak flux, when striking the aluminum pipe at a small angle, was reflected into the ½-in.×2-in. defining counter. A symmetrized subtraction of this reflection was made for the high-energy continuum points, and amounted to about a 10% correction.

The data pertaining to reaction (2), that is the three peaks, were analyzed by integrating under each peak after assuming it to be symmetrical about its center line, and then dividing the result by the counter width. Figure 6 shows the 30° peak and continuum beginning, and illustrates the high degree of symmetry of the peak down to about 40% of maximum, when the continuum begins to distort the peak towards lower energies. The question of a symmetrical resolution function could not affect the peak analyses, since any asymmetry must be small, ~1%. An effective beam energy of 448.4±0.6 Mev, the energy of the protons after passing through the CH_2 target, was assumed in all of the transformation analyses, and gave agreement with the pion range curves to about 1%, the range curve uncertainty. The 30° peak was 2.2% wide; the 20.5° peak was 1.8%

[20] K. M. Crowe, Nuovo cimento 5, 541 (1957).

TABLE I. Analysis of $p+p \rightarrow \pi^+ + d$. Complete analysis of Reaction (2) after numerical area determination. The columns are as follows: (1) lab angle; (2) and (3) result of area integral and squared error; (4) $A=\%$ telescope absorption; (5) $e^{x/\lambda}$ is the decay correction $x=130''$; (6) $B=\%$ target absorption; (7) $\Delta\Omega$ is lab solid angle; (8) and (9) lab differential cross section in microbarns/sterad and square error; (11) center-of-mass differential cross section in microbarns/sterad.

1 θ	2 N_{π^0}	3 ϵ_{π^2}	4 (N^0+AN^0) N_1	5 $e^{x/\lambda}N$ N_2	6 (N_2+BN_2) N_3	7 $N_3/\Delta\Omega$	8 $d\sigma/d\Omega$	9 ϵ_{tot^2}	10 $d\Omega/d\bar{\Omega}$	11 $d\sigma/d\bar{\Omega}$
13°46′	2930	32 400	3106	3913	3972	3.34×10^6	645	2044	0.333	215±15
20°27′	2210	10 000	2343	2976	3021	2.38×10^6	459	685	0.353	162± 9
30°14′	1430	7225	1504	1948	1977	1.66×10^6	320	489	0.400	128± 9

wide; and the 14° peak was 1.5% wide. These widths could be explained by considering the following sources: (a) horizontal beam spot size, $\frac{1}{2}$ in.; (b) energy spread of pion beam across 2.3° angular opening of the magnet; (c) width of defining counter, $\frac{1}{2}$ in.; and (d) multiple scattering in the target, contributing to (b). It was not necessary to assume an incident energy spread, and target straggling was not important because pion and proton energy losses in the target tended to cancel. Table I shows the analysis of the reaction (2) data after integration. A least squares fit to the results gave

$$d\sigma/d\Omega \propto (0.38\pm0.20+\cos^2\theta), \quad (5)$$

and

$$\sigma=1.47\pm0.12 \text{ millibarns}. \quad (6)$$

This result agrees well with the excitation function of Crawford and Stevenson,[9] which predicts $\sigma=0.138\eta+1.01\eta^3$ mb$=1.47$ mb for $\eta=1.093$. The total cross section and angular distribution also agree with the results of Fields *et al.* at 437 Mev.[21]

The assumption of a symmetrical resolution function, although valid for the reduction of the peak data, could contribute an error to the high-energy continuum data because of the large peak rate to continuum rate ratio. Nevertheless no low-energy tail was assumed to be present on the peak shape because of the lack of experimental evidence to the contrary. The continua were assumed to rise abruptly to their maximum values at the high-energy end, and this rise was assumed to occur at the mid-point of the rise obtained by subtracting the symmetrized low-energy tail of the peak. This assumption allowed the calculation of deuteron binding energies, which agreed with predictions to 25% or better.

Table II gives the complete analysis of the 30° spectrum data. The corrections were applied to the continuum data in the following sequence. First the estimated muon contamination striking the defining counter was subtracted from the net number of hydrogen counts observed at a given momentum; then the fraction of pions absorbed by the telescope was added, and the number of pions reflected off of the vacuum system was subtracted. Then came the two large correction factors: the counter resolution factor and the pion decay correction, both of which were well known, however. The transformation of the differential cross section into the center of mass was effected by using the invariance of $(1/p)(d^2\sigma/dEd\Omega)$. Figure 7 shows the three lab spectra after all corrections have been applied except the transformation into the center of mass. The maximum center-of-mass energies were 64.0, 64.5, and 66.0 Mev, in order of increasing lab angle. The calculated end point energy for the continuum in the center of mass was found to be 64.9 Mev. The ~1 Mev scatter was eliminated by shifting the spectra near the high-energy end so that each spectrum began at 64.9 Mev.

B. Comparison of the Results

The four phenomenological model spectrum shapes shown in Fig. 8 were used in an attempt to make a

TABLE II. Continuum data analysis for 30°14′. The following columns require explanation: (4) $n\mu$ is the μ meson contamination as estimated from calculations. It is assigned a 100% error; (5) $A=\%$ telescope absorption; (6) n_π is the reflection effect of the peak off of the exit vacuum pipe; (7) ΔE is the defining counter width in Mev; (9) ϕ is the decay correction factor; (11) $B=\%$ target absorption; (12) lab cross section in microbarn/Mev sterad; (13) $\bar{p}=$center of mass momentum of pion; (14) and (15) center-of-mass cross section in microbarn/Mev sterad; (16) center-of-mass angle.

1 Mev/c p_π	2 N_{π^0}	3 ϵ^2	4 $(N^0-n\mu)$ N_1	5 (N_1+AN_1) N_2	6 (N_2-n_π) N_3	7 $(1/\Delta E)$	8 $(1/\Delta E)N_3$ N_4	9 ϕ	10 ϕN_4	11 (N_5+BN_5)	12 lab $d^2\sigma/dEd\Omega$	13 $\bar{p}/p$	14 c.m. $d^2\sigma/dEd\Omega$	15 ϵ^2	16 θ
236	0	3969	−3	−3	−3	0.725	−2	1.30	−3	−3	0	0.640	0	0.529	52.2°
232.5	567	1108	564	589	539	0.741	399	1.30	519	525	9.45	0.639	6.04	0.336	52.2°
230.5	540	1068	537	561	511	0.746	381	1.305	497	502	9.04	0.642	5.80	0.326	52.4°
229	567	1079	564	586	539	0.752	405	1.31	530	536	9.65	0.637	6.15	0.349	52.4°
208.5	244	319	242	251	251	0.855	215	1.345	289	292	5.26	0.626	3.29	0.110	53.5°
194	204	270	202	209	209	0.934	195	1.370	267	269	4.84	0.618	2.99	0.102	54.6°
174	150	110	148	153	153	1.093	167	1.420	237	239	4.30	0.606	2.60	0.067	56.6°
162	100	59	98	101	101	1.200	121	1.460	177	178	3.20	0.596	1.91	0.048	58.0°
142	61	68	59	61	61	1.460	89	1.530	136	137	2.47	0.577	1.42	0.058	64.1°
117	32	47	31	32	32	1.972	63	1.690	106	107	1.93	0.538	1.04	0.058	66.4°

[21] Fields, Fox, Kane, Stallwood, and Sutton. Phys. Rev. **109**, 1704 (1958).

detailed comparison of the theory with the observed energy and angular distribution. These spectra are proportional to the following expressions:

$$Ss: \frac{d\sigma}{dT} \propto \frac{\eta(T_0-T)^{\frac{1}{2}}}{B+(T_0-T)}, \tag{7}$$

$$Sp: \frac{d\sigma}{dT} \propto \frac{\eta^3(T_0-T)^{\frac{1}{2}}}{B+(T_0-T)}, \tag{8}$$

$$Ps: \frac{d\sigma}{dT} \propto \eta(T_0-T)^{\frac{3}{2}}, \tag{9}$$

$$Pp: \frac{d\sigma}{dT} \propto \eta^3(T_0-T)^{\frac{3}{2}}, \tag{10}$$

where η is the pion momentum in units of mc, B is the deuteron binding energy, and T, T_0 represent the pion energy and maximum pion energy respectively. The normalizing integrals, Λ, have the following values:

$$\begin{aligned} &\Lambda_{Ss}=8.98\ (\text{Mev})^{\frac{1}{2}}, \quad \Lambda_{Ps}=6720\ (\text{Mev})^{\frac{5}{2}}, \\ &\Lambda_{Sp}=6.64\ (\text{Mev})^{\frac{1}{2}}, \quad \Lambda_{Pp}=2650\ (\text{Mev})^{\frac{5}{2}}. \end{aligned} \tag{11}$$

The cross sections plotted in Fig. 8 are the shapes given by Eqs. (7) through (10), each divided by the appropriate normalizing Λ. Following the angular momentum analysis of the various states as discussed by Rosenfeld,[1] the differential cross section can be written as:

$$\frac{d^2\sigma}{dEd\Omega} = \alpha_1 \left.\frac{d\sigma}{dT}\right|_{Ss} + \alpha_2 \left.\frac{d\sigma}{dT}\right|_{Ps} + \alpha_3 \left.\frac{d\sigma}{dT}\right|_{Sp} + \alpha_4 \left.\frac{d\sigma}{dT}\right|_{Pp} + \left\{ \alpha_5 \left.\frac{d\sigma}{dT}\right|_{Sp} + \alpha_6 \left.\frac{d\sigma}{dT}\right|_{Pp} \right\} \cos^2\theta, \tag{12}$$

where the α's are unknown parameters. According to our

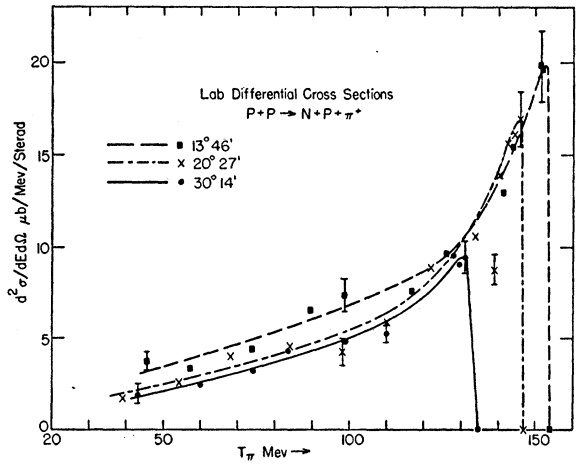

FIG. 7. Laboratory differential cross sections for the three angles. Only representative errors are shown.

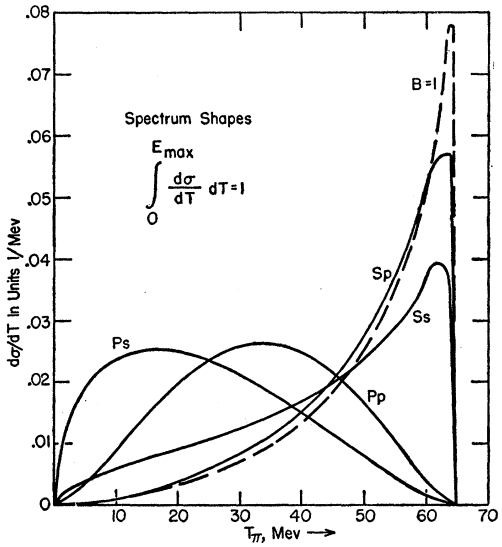

FIG. 8. The four phenomenological spectrum shapes used in the least squares fit. The dashed curve represents the Sp spectrum if $B=1$ Mev rather than 2.2 Mev.

normalization the total cross section is

$$\sigma = 4\pi\{\alpha_1+\alpha_2+\alpha_3+\alpha_4+\tfrac{1}{3}(\alpha_5+\alpha_6)\}. \tag{13}$$

Let us write Eq. (12) in the form $y=\sum_j \alpha_j f_j(x,\theta)$, where $f_1(x,\theta)=d\sigma/d\Omega|_{Ss}$, etc.; and x is the pion energy. In this form the standard least squares technique was used to calculate the α's. Following the analysis of Solmitz,[22] we calculated by hand a 6×6 matrix G and a 6 element vector ζ, from which the experimental values α^* could be found from $\alpha^*=G^{-1}\zeta$. Table III gives G and ζ. The matrix was inverted by George, a computer at the Argonne National Laboratory, and it was discovered that G was nearly singular, resulting in a poorly determined inverse. To study the problem further, George was asked to diagonalize G, and to find the unitary matrix S, such that $G'=\tilde{S}GS$. Table IV lists the eigenvalues of G' and gives the matrix S. Note that the last eigenvalue of G' is almost a factor 10^3 smaller than any of the other eigenvalues, and is, to the accuracy of the calculation, zero. In the diagonal frame, the coefficients α_j' are given by $\alpha_j'=\zeta_j'/G_j'$, with $\langle\Delta\alpha_j'^2\rangle_{Av}=1/G_j'$. The element $G_6'=0$ because the expression $\sum_i S_{i6}f_i(x,\theta)=0$. This term is in fact down by a factor 10^2 from the f's themselves. Call the coefficient of this sum, which belongs to G_6', k. Then the coefficients α' can be solved for, and the desired coefficients α can be found by a transformation:

$$\begin{aligned} \alpha_1' &= 88.622, & \alpha_1 &= 15.883+0.8066k, \\ \alpha_2' &= 51.567, & \alpha_2 &= 30.883-0.1068k, \\ \alpha_3' &= 13.808, & \alpha_3 &= 18.246-0.5652k, \\ \alpha_4' &= -108.61, & \alpha_4 &= 14.717-0.1347k, \\ \alpha_5' &= -106.09, & \alpha_5 &= 177.993+0.0194k, \\ \alpha_6' &= k, & \alpha_6 &= 16.848-0.0079k. \end{aligned} \tag{14}$$

[22] Frank T. Solmitz (unpublished).

TABLE III. Error matrix and vector. (ζ in units of μb/Mev sterad.)

$$G=\begin{bmatrix} 0.08602 & 0.05774 & 0.09795 & 0.06433 & 0.05515 & 0.03271 \\ & 0.12541 & 0.03451 & 0.10110 & 0.01759 & 0.04994 \\ & & 0.12388 & 0.04813 & 0.07073 & 0.02497 \\ & & & 0.10364 & 0.02498 & 0.05184 \\ & & & & 0.04395 & 0.01476 \\ & & & & & 0.03027 \end{bmatrix}; \qquad \zeta=\begin{bmatrix} 16.193 \\ 10.928 \\ 18.823 \\ 11.935 \\ 11.212 \\ 6.441 \end{bmatrix}$$

The coefficients have units of microbarns. To a good approximation only S_{16} and S_{36} are nonzero. If we make this assumption, the solution is:

$$\begin{aligned} 0.5652\alpha_1+0.8066\alpha_3 &= 23.69\pm 9.25\ \mu\text{barn}, \\ \alpha_2 &= 30.8 \pm 8.0\ \mu\text{barn}, \\ \alpha_4 &= 14.72\pm 12.1\ \mu\text{barn}, \\ \alpha_5 &= 177.9 \pm 18.9\ \mu\text{barn}, \\ \alpha_6 &= 16.8 \pm 15.7\ \mu\text{barn}. \end{aligned} \tag{15}$$

The errors here were computed, as they will be in each case, by using the uncorrelated errors of the α' elements, except for k, and the transformation matrix S. We shall always assume, in calculating errors, that α_1 and α_3 appear in the linear combination shown above, and that this combination eliminates k and its accompanying infinite error.

The functions f_1 and f_3 are indistinguishable in this experiment because of their similar shape, and identical angular distribution, and because of the large $\cos^2\theta$ dependence of the high energy parts of the spectra. In order to separate these two terms, the excitation function of the total cross section should be investigated, since $\Lambda_{Ss}\sim\eta$ and $\Lambda_{Sp}\sim\eta^4$ in energy dependence. The phenomenological theory can be used, however, to predict α_1, and a comparison between theory and experiment can be made. According to the theory the Ss state is related to s state production in reaction (2), and the Sp state is related to p state production in the following manner:

$$\frac{\sigma(n+p,\,Ss)}{\sigma(d,s)}=\frac{\Lambda_{Ss}}{2\pi(B)^{\frac{1}{2}}\eta'}, \tag{16}$$

$$\frac{\sigma(n+p,\,Sp)}{\sigma(d,p)}=\frac{\Lambda_{Sp}}{2\pi(B)^{\frac{1}{2}}\eta'^3}, \tag{17}$$

where η' is the momentum of the pion from reaction (2). Now at $\eta'=1.09$, $\sigma(d,s)=0.151$ millibarn, and $\sigma(d,p)=1.32$ millibarns, so that we predict

$$\begin{aligned} \alpha_1 &= 10.5\ \mu\text{barn}, \\ (\alpha_3+\tfrac{1}{3}\alpha_5) &= 57\ \mu\text{barn}. \end{aligned} \tag{18}$$

If $\alpha_1=10.5$ μbarn, then from Eq. (15) we find

$$(\alpha_3+\tfrac{1}{3}\alpha_5)=81.2\pm 4.0\ \mu\text{barn}. \tag{19}$$

This result is to be compared with the predicted value of 57 ± 6 μbarns given in Eq. (18).

Figure 9 shows the fit obtained from Eq. (15) with $\alpha_1=10.5$ μbarns. The result is, of course, insensitive to the choice of α_1 over a reasonably wide region. The value of χ^2 for this fit is 143, which is excessively large for a fit of 29 degrees of freedom. The very low datum at 60 Mev contributes about 60 to χ^2 and the various points above the curve at 62 Mev contribute about 50 to χ^2, which explains its unusually large magnitude. Because of the very small tail needed on the resolution function to bring the cluster of 62 Mev points down, it is impossible to say whether this effect is real or not. If we assume that it is real, then the agreement between Eqs. (19) and (18), as well as the fit at 62 Mev, can be improved. Rosenfeld has suggested that the pion-nucleon interaction might manifest itself at low energies through a decrease in the deuteron binding energy which appears in the denominator of the Ss and Sp spectrum shapes as a consequence of effective range theory.[1] To test this idea Ss and Sp spectra with $B=1$ Mev rather than 2.2 Mev were investigated. These spectra have different normalization integrals; the new values are $\Lambda_{Ss}=9.91$ (Mev)$^{\frac{1}{2}}$ and $\Lambda_{Sp}=7.57$ (Mev)$^{\frac{1}{2}}$. Using these numbers and Eqs. (16) and (17) we obtained new predictions for the Ss and Sp cross sections. These results are as follows:

$$\begin{aligned} \alpha_1 &= 12.0\ \mu\text{barn}, \\ (\alpha_3+\tfrac{1}{3}\alpha_5) &= 79.5\ \mu\text{barn}. \end{aligned} \tag{20}$$

The agreement between the prediction and Eq. (19) is clearly improved. In fact letting $\alpha_1=12.0$ μbarns leads to

$$(\alpha_3+\tfrac{1}{3}\alpha_5)=80.3\pm 4.0\ \mu\text{barns}. \tag{21}$$

TABLE IV. Eigenvalues of the error matrix and the unitary transformation.

$$\begin{aligned} G_1'&=0.35593 \\ G_2'&=0.13744 \\ G_3'&=0.01357 \\ G_4'&=0.00458 \\ G_5'&=0.00161 \\ G_6'&=0.000004 \end{aligned} \qquad S=\begin{bmatrix} 0.46463 & 0.25484 & 0.04348 & 0.20124 & 0.16191 & 0.80657 \\ 0.46523 & -0.55481 & 0.67145 & -0.11332 & 0.03173 & -0.10679 \\ 0.46947 & 0.57327 & 0.08090 & 0.20902 & 0.28590 & -0.56519 \\ 0.46863 & -0.37835 & -0.57903 & 0.36826 & -0.38352 & -0.13473 \\ 0.26286 & 0.34972 & 0.03941 & -0.60187 & -0.66633 & 0.01944 \\ 0.24197 & -0.18202 & -0.45153 & -0.63646 & 0.54766 & -0.00791 \end{bmatrix}$$

A new fit with these spectra was not attempted, but an idea of the possible improvement can be ascertained from the properly normalized $B=1$ Sp spectrum in Fig. 8. The total cross section, assuming $\alpha_1=10.5$ μbarn, is

$$\sigma=1.80\pm0.07 \text{ millibarns.} \quad (22)$$

This 4% error is derived by adding statistical and beam monitor errors quadratically, assuming Eqs. (15). Varying α_1 from 0 to 20 μbarn does not change σ outside the quoted error. After integrating over energy, the cross section is given by $d\sigma/d\Omega \propto A+\cos^2\theta$. For $\alpha_1=10.5$ μbarn, we have

$$A=0.40\pm0.08, \quad (23)$$

with a ±0.02 variation for 0 to 20 μbarn change in α_1. The dependence of A on η predicted by these results is shown in Fig. 10.

The total contribution from P-wave nucleon states can be found independent of our value of α_1, assuming that Eq. (15) is justified. This equation gives us the

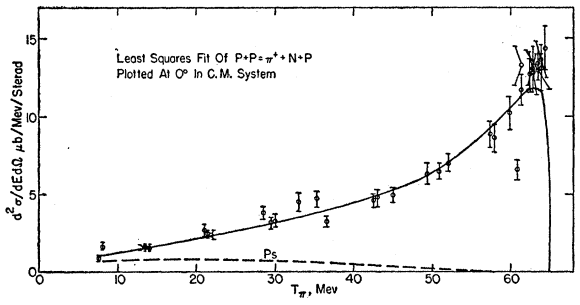

FIG. 9. Results of the least squares fit assuming $\alpha_1=10.5$ μbarns. All data have been projected onto 0° in the center of mass. The dotted curve represents $\alpha_2 Ps$.

following directly:

$$\sigma_{10}(Pp)+\sigma_{11}(Pp)=0.25\pm0.11 \text{ mb}, \quad (24)$$

$$\sigma_{11}(Ps)=0.39\pm0.10 \text{ mb}. \quad (25)$$

These results are to be compared with the measured excitation function for reaction (4). Moyer and Squire,[11] working from 327 Mev to 342 Mev, report

$$\sigma_{11}=0.02\eta^2+(0.57\pm0.11)\eta^8 \text{ mb}. \quad (26)$$

The η^2 term belongs to class Ss, and contributes only 20 microbarns to the cross section at our energy; it is too small to be seen in this experiment. Stallwood *et al.* measured reaction (4) from 346 Mev to 437 Mev, and included the lower energy results of Moyer and Squire in their analysis.[12] Their best result is

$$\sigma_{11}=[(0.027)\pm0.010)\eta^2 + (0.075\pm0.070)\eta^8] \text{ millibarns}. \quad (27)$$

They obtain a somewhat worse fit by replacing the η^8 term with $(0.062\pm0.015)\eta^6$. This solution was ruled out by the authors because it belongs to Ps, which must be

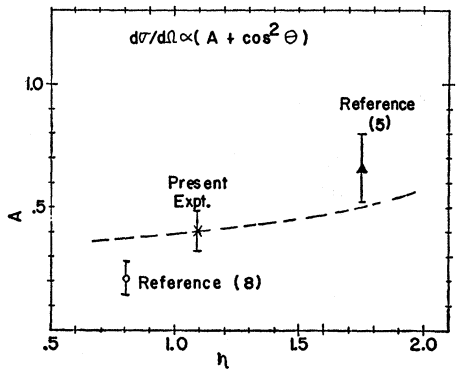

FIG. 10. Momentum dependence of the isotropic term in the angular distribution.

isotropic. It has been pointed out by Mandelstam, however, that displaced D state production can be large in σ_{11} near threshold, and can lead to anisotropy with an η^6 dependence.[23] The total cross sections reported by Stallwood fit smoothly to the higher energy work of Prokoshkin and Tyapkin,[24] and lead to a cross section of $\sim$180 microbarns at 450 Mev. Equation (26) has much too large an η^8 coefficient. Combining (27) and (24) we have

$$\sigma_{10}(Pp)=0.10\pm0.11 \text{ millibarn}, \quad (28)$$

or

$$\sigma_{10}(Pp)\approx(0.05\pm0.05)\eta^8 \text{ millibarn}. \quad (29)$$

This amount is much less than that conjectured by Alston *et al.*[8] Their best value would predict $\sigma_{10}(Pp)\approx2.8$ millibarns at our energy, which is larger than our total cross section. Fields *et al.*[25] also reports a much smaller value of $\sigma_{10}(Pp)$ at 437 Mev, on the basis of a total cross section measurement.

Figure 11 shows the excitation function predicted by the solution (15) with $\alpha_1=10.5$ microbarns. The curve was obtained by numerical evaluation of the spectrum integrals at various energies. The predicted curve agrees well with the 383-Mev datum of Alston *et al*, but increases too rapidly with η to account for the Russian data, especially at energies above 560 Mev. The weighted mean of the results of Dzhelepov, *et al*[4] and of Neganov and Savchenko,[5] would be below our curve over the whole range above 500 Mev. A major factor in this increase is contributed by the Ps coefficient and spectrum integral, since the former is large, and the latter increases roughly as η^6.

A comparison of Eqs. (25) and (27) shows that the Ps term required to fit our experimental data is larger than the total cross section $\sigma_{11}\approx180$ microbarns at 450 Mev. This discrepancy might be resolved by allowing higher nucleon angular momentum states to enter the

[23] S. Mandelstam (private communication).
[24] I. D. Prokoshkin and A. A. Tyapkin, J. Exptl. Theoret. Phys. U.S.S.R. **32**, 750 (1957) [translation: Soviet Phys. JETP **5**, 618 (1957)].
[25] Fields, Fox, Kane, Stallwood, and Sutton, Phys. Rev. **109**, 1713 (1958).

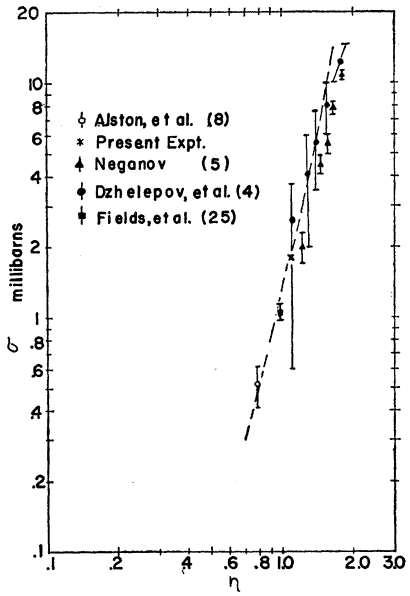

FIG. 11. Momentum dependence of the total cross section. The dashed curve represents the prediction of the phenomenological theory.

problem. For example the *Ds* spectrum, which comes from the ^3F initial state, is isotropic, has an energy distribution proportional to $\eta(T_0-T)^{\frac{5}{2}}$, and is similar in shape to the *Ps* spectrum. In addition, this spectrum can occur in σ_{10}. About 10% of the total production cross section would have to be due to *D*-wave nucleon motion, however, which seems excessive in the light of *p-p* polarization data.[26] In addition, the *Ds* spectrum would increase $\sim\eta$,[8] giving an even more steeply rising excitation function at high energies.

IV. CONCLUSIONS

Our measurement of the unbound positive pion spectrum produced by 450-Mev protons in hydrogen has been compared to the phenomenological theory first proposed by Brueckner and Watson. Agreement between theory and experiment was found to be generally good for *p* wave pions, and the connection with the deuteron formation cross section. An increase in the *np* scattering length to give an effective binding energy $B=1$ Mev improves this agreement, but should not be considered seriously because of experimental uncertainty. The amount of the *Ps* spectrum shape required by our least squares fit is quite large, and presents a problem regarding its interpretation in terms of the phenomenological model. The introduction of higher angular momentum states does not seem to resolve this discrepancy. It is possible, however, that further investigations of the π^0 spectrum may indicate a larger amount of *Ps* than previously reported.[27] The excitation function for reaction (1) predicted by the phenomenological theory on the basis of the results of this experiment rises too steeply at high energies, above 500 Mev. The comparison between $\sigma_{10}(d)$ and $\sigma_{10}(n+p)$ is based principally on the high-energy part of the spectrum, which is strongly angular dependent. The contradictions arise in the lower half of the spectrum, where our measurements indicate a large number of pions and a high degree of isotropy. The phenomenological model combined with the present data does not seem to account successfully for this region.

ACKNOWLEDGMENTS

The author wishes to acknowledge the aid of Professor U. E. Kruse, under whose sponsorship this work was performed, and the continued assistance and encouragement of Professor A. V. Crewe, who furnished invaluable advice. Doctor Brian Ledley assisted in taking the experimental data. Thanks are due to Mr. R. Hoff for aid in the calculations, and to Mr. Burton J. Garbow of the Argonne National Laboratory for his cooperation in inverting and diagonalizing the error matrices on George. We also wish to thank Mr. Clovis A. Bordeaux and the cyclotron crew for the efficient machine operation during the four weeks of the final run.

[26] L. Wolfenstein, *Annual Reviews of Nuclear Science* (Annual Reviews, Inc., Stanford, 1956), Vol. 6, p. 43.

[27] Carl M. York (private communication).